

Constraining the evolution of stellar rotation using solar twins

Diego Lorenzo-Oliveira,^{1*} Jorge Meléndez,¹ Jhon Yana Galarza,¹ Geisa Ponte²,
Leonardo A. dos Santos³, Lorenzo Spina⁴, Megan Bedell⁵, Iván Ramírez⁶,
Jacob L. Bean⁷ and Martin Asplund⁸

¹Universidade de São Paulo, Departamento de Astronomia do IAG/USP, Rua do Matão 1226, Cidade Universitária, 05508-900 São Paulo, SP, Brazil

²Universidade Federal do Rio de Janeiro, Observatório do Valongo, Ladeira do Pedro Antonio 43, CEP: 20080-090 Rio de Janeiro, RJ, Brazil

³Observatoire astronomique de l'Université de Genève, 51 chemin des Maillettes, 1290 Versoix, Switzerland

⁴Monash Centre for Astrophysics, School of Physics and Astronomy, Monash University, VIC 3800, Australia

⁵Center for Computational Astrophysics, Flatiron Institute, 162 5th Ave., New York, NY 10010, USA

⁶Tacoma Community College, 6501 South 19th Street, Tacoma, Washington 98466, USA

⁷University of Chicago, Department of Astronomy and Astrophysics, USA

⁸The Australian National University, Research School of Astronomy and Astrophysics, Cotter Road, Weston, ACT 2611, Australia

Accepted XXX. Received YYY; in original form ZZZ

ABSTRACT

The stellar Rotation *vs.* Age relation is commonly considered as a useful tool to derive reliable ages for Sun-like stars. However, in the light of *Kepler* data, the presence of apparently old and fast rotators that do not obey the usual gyrochronology relations led to the hypothesis of weakened magnetic braking in some stars. In this letter, we constrain the solar rotation evolutionary track using solar twins. Predicted rotational periods as a function of mass, age, [Fe/H] and given critical Rossby number (Ro_{crit}) were estimated for the entire rotational sample. Our analysis favors the smooth rotational evolution scenario and suggests that, if the magnetic weakened breaking scenario takes place at all, it should arise after $Ro_{\text{crit}} \gtrsim 2.29$ or ages $\gtrsim 5.3$ Gyr (at 95% confidence level).

Key words: Sun: rotation – stars: solar-type – stars: rotation – stars: fundamental parameters

1 INTRODUCTION

Rotation-based ages of old Sun-like stars are rooted in a complex and intricate dependence on age, rotation, turbulent convection, structural variations and mass-loss due to magnetized winds (Skumanich 1972; Reiners & Mohanty 2012; Guerrero et al. 2013; O’Fionnagáin & Vidotto 2018). Classically, the age-dating method that relies on this phenomenon assumes that the rotational periods (P_{rot}) can be expressed in well-defined functions of the age and mass (or a proxy of it), the so-called gyrochronology relations (Barnes 2007; Mamajek & Hillenbrand 2008). These relations had successfully confirmed the paradigm of rotation-activity-age coupling that powers the global dynamo evolution along the main-sequence (Barnes 2007; Vidotto et al. 2014; do Nascimento et al. 2014; Lorenzo-Oliveira et al. 2016, 2018) and

reproduced the main features observed in open clusters spanning a wide range of ages (Meibom et al. 2015).

Apart from this inspiring agreement, some of the old *Kepler* field stars shows unexpected fast rotation, especially hotter ones with ages greater than 2–3 Gyr (Angus et al. 2015; Metcalfe et al. 2016). This tension led to idea that after a critical Rossby number ($Ro \equiv P_{\text{rot}}/\tau_{\text{CZ}}$, where τ_{CZ} is the convective turnover time; Noyes et al. 1984) a drastic change of the stellar differential rotation (SDR) pattern might hamper the production and maintenance of magnetic field large-scale components over secular timescales. One of the most important (and accessible) effects of this drastic transition would be the presence of old and fast rotating stars with reduced angular momentum loss caused by magnetized winds. However, recent observational results gave us alternative hints about the possible smooth nature of the Sun-like rotational evolution in the light of *Kepler* asteroseismic data (Benomar et al. 2018).

* E-mail: diegolorenzo@usp.br

Motivated by this up-to-date discussion about the smooth nature of the age-rotation relations, we can ask ourselves: *what solar twins can tell us about the solar rotational evolution?* This letter uses solar twins to evaluate a recent claim (van Saders et al. 2016) about the solar rotational transition at a given critical Rossby number. Sec. 2 describes our working sample, selection criteria of solar twin rotators and determination of P_{rot} through activity time series. In Sec. 3 we discuss the age-rotation evolution of solar twins and the suitability of standard rotational evolution models. The conclusions are drawn in Sec. 4.

2 SOLAR TWINS ROTATION SAMPLE

We compiled 79 solar twins (plus the Sun) presented in Spina et al. (2018). Our sample was extensively observed over the years (2011–2016) with HARPS spectrograph (Mayor et al. 2003) fed by the 3.6 m telescope at La Silla Observatory, to search for planets around solar twins (program 188.C-0265, Meléndez et al. 2017). To prevent the inclusion of anomalously fast rotators due to binarity effects, 17 spectroscopic binary (SB) stars and other solar twins with a close companion within $4''$ were discarded from the analysis (dos Santos et al. 2017). Other interesting solar twins spectroscopically analyzed in the past by our group were added to our sample (HIP30503 and HIP78399 in Galarza et al. 2016). The resulting HARPS sample of this work is composed of 65 stars.

In order to estimate rotational velocities and other stellar parameters of interest, we made use of the updated atmospheric parameters (T_{eff} , $\log g$, $[\text{Fe}/\text{H}]$, and $[\alpha/\text{Fe}]$) provided by Spina et al. (2018). *Gaia* DR2 G band photometry and parallaxes (*Gaia* Collaboration et al. 2018) were combined to the spectroscopic data to obtain stellar ages, masses, $\log g$ and other evolutionary parameters following the procedures described in Grieves et al. (2018) (see their Sec. 6). For distant *Kepler* solar twins that will be described in the following sections, we used the reddening G band corrections provided by *Gaia* DR2. The typical mass and metallicity of our solar twin sample agrees with solar parameters within $\pm 0.05 M_{\odot}$ and ± 0.04 dex, respectively. Stellar atmospheric and evolutionary parameters, projected P_{rot} and other relevant information of the entire sample is shown in Table 1. Projected rotational and macroturbulence velocities were determined through HARPS *full width half maximum* of the *cross correlation function* ($FWHM_{\text{CCF}}$) vs. $v \sin i$ together with macroturbulence calibrations provided by dos Santos et al. (2016). For details about the adopted procedures, see their Sec. 3. The CCF based $v \sin i$ errors are computed propagating the $FWHM_{\text{CCF}}$ calibration and typical $v \sin i$ measurement errors estimated by dos Santos et al. (2016) yielding $\sigma(v \sin i) = 0.23$ km/s or $\sigma(P_{\text{rot}}/\sin i)$ of 3 days (assuming 2% of $\sigma(R/R_{\odot})$).

Given that the rotation axes of the stars are randomly oriented in different inclination angles (i), our spectroscopic analysis is limited by the projection factor $\sin i$ (Gray 2005). This feature skews the P_{rot} distribution towards higher values of rotation for a given age owing to the geometric factor $1/\sin i$. On the other hand, if one analyses a progressively larger sample of stars, it is indeed expected that, for a given age/mass/ $[\text{Fe}/\text{H}]$, the lower boundary of $P_{\text{rot}}/\sin i$ distribution asymptotically matches with the *true* distribution of P_{rot} which is scattered by intrinsic effects (e.g. propagation

of initial conditions and SDR effects). In fact, this approximation has an optimal applicability for samples of twin stars like ours, where mass and $[\text{Fe}/\text{H}]$ effects, that might hamper the statistical corrections towards the true P_{rot} distributions, are mitigated.

Through 10^6 Monte-Carlo (MC) simulations we sought for an optimal selection criterion that closely unveils the distribution of stars with the highest chance of having $\sin i \sim 1$, for a given sub-sample size N . We ran N MC simulations assuming random angle orientations ranging from 0 to $\pi/2$ for a range of angular rotational frequencies (Ω). We assigned an intrinsic Ω error of 10% to account for stellar differential rotation (SDR, Epstein & Pinsonneault 2014). For each simulation, the difference (Δ) between the *true* P_{rot} and the median $P_{\text{rot}}/\sin i$ distribution delimited by its upper 0.5(P50), 0.7(P70), 0.84(P84), and 0.975(P98) percentiles cut-offs. This procedure was repeated 10^4 times in order to estimate the best selection criteria (using the sample medians of each upper percentiles cut-offs) that minimizes $|\Delta|$ – i.e. the stellar inclination selection bias. For a typical sub-sample size of 10 stars, we found that the average between P70 and P98 estimates closely converges into the centroid of the *true* P_{rot} distribution, assuming rotation roughly constant along the age domain considered. The exclusion of the upper 2.5% of each simulation prevents to systematically include unusually fast-rotating stars in each age-bin. Following this selection prescription, we bootstrapped the 1σ confidence intervals within each age-bin of 2 Gyr through 10^4 repetitions. We found 2 Gyr age-bin as our optimal choice because it balances sampling and the ratio between the expected P_{rot} evolution and realistic P_{rot} errors due to intrinsic effects, at least for stars older than ~ 1 Gyr. In fact, during the simulations, we also compute the age- P_{rot} correlation within each age bin and found negligible correlation between both variables (p-value $\gg 0.05$). In Table 1, we highlight the stars with probable $\sin i \sim 1$ along each age-bin. In Fig. 1 (left panel) we show our subsample of 10 stars with both HARPS $P_{\text{rot}}/\sin i$ and P_{rot} measurements. Our $P_{\text{rot}}/\sin i$ estimates are consistent with the 1:1 relation represented by the red dashed lines. The intrinsic errors associated to P_{rot} measurements (10%) are given by shaded region along the 1:1 identity line. As the inclination factor is encapsulated in the $P_{\text{rot}}/\sin i$, the projected P_{rot} are slightly shifted towards higher rotation values albeit it marginally converges into the shaded region indicating that the majority of these stars have $\sin i \sim 1$.

Using our large Ca II activity time-series of solar twins (Lorenzo-Oliveira et al. 2018), we determined P_{rot} of six stars using a Generalized Lomb-Scargle analysis (GLS, Zechmeister & Kürster 2009): HIP 1954, 30503, 36515, 79672, 95962 and 118115. Our procedure is similar to the one described by Suárez Mascareño et al. (2017). In brief, for each star, we cleaned our time-series by removing the observations with low signal to noise ratio around the Ca II lines ($\text{SNR} < 30$). To avoid the inclusion of poor observations or stellar transient events such as flares, we removed from the activity time-series outliers placed above $\geq 2.5\sigma$. Then, we look for the presence of strong signals with bootstrapped false-alarm probability (FAP) $\geq 3\sigma$ at frequencies related to typical rotational timescales (≤ 50 days). In other cases where no significant peaks were found, we detrended the time-series from eventual sinusoidal long-term signal (FAP $\geq 3\sigma$) that are

Table 1. Relevant parameters for our rotation sample of solar twins stars analyzed in this paper. This table is available in its entirety in machine readable format at the CDS.

HIP	Age [Gyr]	Mass [M/M_{\odot}]	[Fe/H]	$P_{\text{rot}}/\sin i$ [d]	P_{rot} [d]	P_{rot}^P [d]	$P_{\text{rot}}^P(Ro_{\text{crit}} = 2.0)$ [d]	Remark
1954	$4.3^{+0.3}_{-0.3}$	0.97 ± 0.03	-0.090 ± 0.003	26.6 ± 3.1	24.1 ± 0.2	25.2 ± 2.7	24.8 ± 2.7	This work
7585	$4.1^{+0.3}_{-0.3}$	1.03 ± 0.03	0.083 ± 0.003	24.1 ± 3.0	23.0 ± 2.3	23.4 ± 3.4	20.3 ± 3.9	See et al. (2017)
22263	$0.6^{+0.2}_{-0.2}$	1.06 ± 0.03	0.037 ± 0.006	14.8 ± 3.0	11.8 ± 3.0	9.6 ± 4.3	9.6 ± 4.3	Suárez Mascareño et al. (2017)
30503	$3.0^{+0.7}_{-0.7}$	1.08 ± 0.04	0.070 ± 0.016	27.3 ± 3.0	20.0 ± 0.1	18.7 ± 4	15.6 ± 3.8	This work
36515	$0.3^{+0.3}_{-0.3}$	1.03 ± 0.03	-0.029 ± 0.009	11.9 ± 3.0	4.6 ± 1.2	7.2 ± 2.3	7.2 ± 2.3	This work

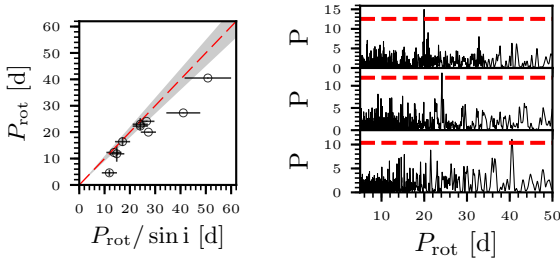


Figure 1. *Left panel:* Comparison between P_{rot} and $P_{\text{rot}}/\sin i$ for a subsample of 10 solar twins observed by HARPS. The dashed red line stands for 1:1 relation and shaded region represents 10% of P_{rot} intrinsic errors. *Right panels:* Ca II periodogram analysis of three solar twins with different ages. The most probable peaks for HIP30503 (upper panel), HIP1954 (middle panel), and HIP118115 (lower panel) are 20.0, 24.1, and 40.5 days. The dashed red lines stand for the false-alarm probability of 3 sigma.

likely to be associated to stellar cycle modulations. In these cases, the P_{rot} measurements are determined in subsequent periodogram analysis of the detrended time-series. Signals matching with the expected window function in period space were not considered in our analysis. Figure 1 (right panels) shows our periodogram analysis for three solar twins. Rotation periods for another four solar twins were gathered from the literature: HIP 7585, 22263, 42333 and 43297 (Petit et al. 2008; Wright et al. 2011; Suárez Mascareño et al. 2017; See et al. 2017).

Additionally, another four solar twins with *Kepler* P_{rot} were added to our analysis. Precise atmospheric parameters were obtained with Gemini/GRACES (ID:GN-2018B-FT-101) and KECK/HIRES high signal-to-noise ratio and high resolution observations conducted by our group (Bedell et al. 2017, Yana Galarza et al. in prep.): Kepler-11, KIC 10130039, 12404954 and 7202957 (McQuillan et al. 2013; Mazeh et al. 2015). The relevant information about the *Kepler* solar twins are summarized in Table 1. Finally, we collected literature data from three solar metallicity old open clusters observed by the *Kepler* mission spanning a critical age range of rotational evolution: NGC6811 (~ 1 Gyr, $N=5$ stars) NGC6819 (~ 2.5 Gyr, $N=5$ stars) and M67 (~ 4 Gyr, $N=12$ stars) (Meibom et al. 2011, 2015; Barnes et al. 2016; Brandenburg & Giampapa 2018). We restricted our sample selection only to those stars with near-solar T_{eff} based on $(B - V)_0$ index ($5600 \leq T_{\text{eff}} \leq 5900$ K, Casagrande et al. 2010). For NGC6811, the $(B - V)$ colors were estimated inverting the $(g - r)$ vs. $(B - V)$ calibration equation by Bilir

et al. (2005). The average P_{rot} of ~ 1 solar mass star in these clusters are 10.2 ± 0.6 , 18.1 ± 0.5 and 24.0 ± 2.4 days for NGC6811, NGC6819 and M67, respectively.

3 AGE-ROTATION RELATION

In Fig. 2 we highlight the rotational evolution of our sample of selected solar twins (red triangles), open clusters (black squares) and the Sun (in black, represented by the \odot symbol). Stars with measured P_{rot} are represented by the black circles. We denoted as black crosses the centroid of each one of the 2 Gyr age-bin based on its respective age- P_{rot} average and dispersion (see Sec. 2). The solar twin sample is composed of those stars with P_{rot} errors within 1σ from its respective age- P_{rot} cluster centroid. All selected stars are fully consistent with expected dispersion due to intrinsic measurement errors ($\sim 10\%$). The only outlier is the 6 Gyr-old KIC 10130039 which deviates from the expected P_{rot} distribution by more than 50%. Thanks to our extensive radial-velocity monitoring together with detailed mapping of chemical anomalies and activity levels (dos Santos et al. 2017; Spina et al. 2018; Lorenzo-Oliveira et al. 2018), we found that the stars placed considerably below the lower limit of rotation rate for a given age are, in fact, spectroscopic binaries. Two illustrative examples from dos Santos et al. (2016) are the 4.0 and 7.2 Gyr-old SB HIP 19911 and 67620 which rotate at 4.1 km/s and 2.7 km/s level ($P_{\text{rot}}/\sin i \sim 12$ and 20 days), respectively. We found that these stars are not likely to be representative of the rotational sample with a significance higher than 3σ . To test the hypothesis of weakened magnetic braking at a given Rossby number threshold (van Saders et al. 2016), we constructed rotational evolution tracks adopting the well-known modified Kawaler wind-law (assuming $N=1.5$, Kawaler 1988; Krishnamurthi et al. 1997) and the updated YaPSI grid of stellar tracks provided by Spada et al. (2017) for different masses and metallicities. The angular momentum equation is solved assuming a negligible moment of inertia change ($dI/I \rightarrow 0$) along the main-sequence:

$$\frac{dJ}{dt} = -K_w \Omega^3 \left(\frac{R}{R_{\odot}} \right)^{0.5} \left(\frac{M}{M_{\odot}} \right)^{-0.5}, \quad \text{for } \Omega > \Omega_{\text{sat}} \quad (1)$$

The constant K_w is fine-tuned to match the unsaturated rotational evolution model to the solar properties ($P_{\text{rot}} = 25.4$ days at 4.57 Gyr), considering $1.0 M/M_{\odot}$ and solar metallicity track. The saturated value of rotation rate (Ω_{sat}) is

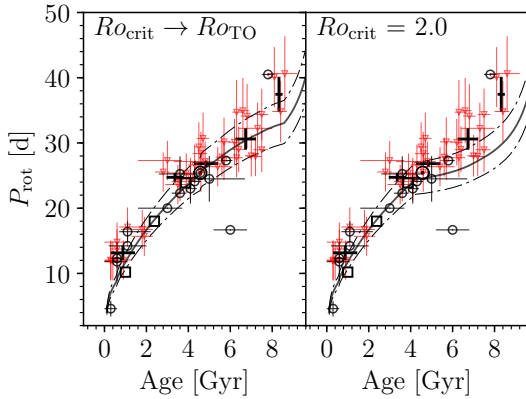


Figure 2. *Left panel:* Modified Kawaler rotation track for 1.00 M_{\odot} and solar metallicity in solid black line without considering the weakened braking efficiency scenario. We assign Ro_{critical} at the turn-off as 2.6 (Ro_{TO}). Dash dotted lines stand for 10% of P_{rot} error given by intrinsic effects. *Kepler* OCs are represented by black squares. Solar twins with measured P_{rot} are the black empty circles. Selected twin sample and its respective age- P_{rot} centroid stand for red triangles and black crosses, respectively. The Sun is represented by \odot . *Right panel:* Modified Kawaler wind law model for $Ro_{\text{critical}}=2.0$.

scaled by the solar convective turnover time following [Krishnamurthi et al. \(1997\)](#). The rotational evolution model is modified whenever the star approaches into the turn-off (TO) region or a given critical Rossby number. After this stage, there is a dominance of structural changes over the magnetic braking terms in the angular momentum evolution (i.e. $dJ/dt \approx 0$). Thus, we fix the angular momentum ($J_{\text{TO/crit}}$), leaving only the moment of inertia to vary towards the main-sequence turn-off ([van Saders & Pinsonneault 2013](#)). For the Sun, our turn-off threshold is at $Ro_{\text{TO}} \gtrsim 2.6$ (or ~ 8 Gyr).

Predicted P_{rot} were derived for 22 Sun-like members of the OCs NGC6811, NGC6819 and M67 using Eq. 1. Effective temperatures were adopted as mass proxy using ($B - V$) calibration by [Casagrande et al. \(2010\)](#) and literature spectroscopic $[\text{Fe}/\text{H}]$ of each OC ([Lee-Brown et al. 2015](#); [Liu et al. 2016](#); [Netopil et al. 2016](#)). In other words, the rotational tracks were built as function of age, T_{eff} and $[\text{Fe}/\text{H}]$. In Fig. 3, we test the consistency of our predicted P_{rot} as a function of T_{eff} , fixing the age of each OC. The 1σ confidence bands set by 10% of P_{rot} uncertainty are represented by the shaded regions around each OC age- T_{eff} diagram prediction. Visually, our predictions are in good agreement with the existent P_{rot} data. For NGC6811, we show a rotational track for an age of 0.85 Gyr which is 15% younger than the canonical age of 1 Gyr.

We show in Fig. 2 the $Ro_{\text{TO}} \sim 2.6$ (left panel) and $Ro_{\text{crit}} \sim 2$ (right panel) scenarios for the rotational evolution of the Sun. Visually, both approaches seem to be in reasonable agreement. The magnetic weakened braking scenario favors the faster rotators placed in the lower boundary of the P_{rot} distribution. On the other hand, the model with smooth rotational evolution follows more closely the average trend observed, especially towards the oldest stars.

We quantified the suitability of both approaches by computing for each star the P_{rot} probability density function that depends on the age, mass, $[\text{Fe}/\text{H}]$ for a given Ro_{crit} .

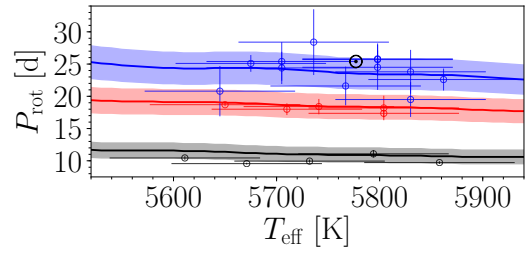


Figure 3. Consistency check of our models using OC data. Blue, red and black lines are the rotational tracks for M67, NGC6819 and NGC6811 with ages of 3.9, 2.4 and 0.85 Gyr, respectively. Each OC is represented by its correspondent color. The Sun is represented by \odot .

The errors are always assumed to follow Gaussian distributions. The adopted theoretical P_{rot} is represented by its median (P_{rot}^P) and 16–84% percentiles based on P_{rot} cumulative distribution function ($\sigma_{P_{\text{rot}}}^P$). For instance, we derived $Ro_{\odot}=2.13$ ($P_{\text{rot},\odot}^P=25.3$ days). We calculated the Bayesian Information Criterion (BIC). BIC accounts the trade-off between the fitting quality (\hat{L}), number of fitting parameters (k) of a given model (M) and the sample size (N): $BIC(M) = -2 \ln \hat{L}(M) + k \ln N$, where $\hat{L}(M)$ is the product of likelihood of each data point with the composite errors computed through quadratic propagation of the individual measured and predicted P_{rot} errors. The BIC difference ($\Delta BIC(M2, M1) \equiv BIC_{M2} - BIC_{M1}$) derived from 2 different models indicates which one is more likely. Defining M1 as the smooth rotational evolution model (Fig. 2, left panel), we calculated $\Delta BIC(M2, M1)$ where M2 stands for models with progressively larger Ro_{crit} ranging from 1.5 up to the subgiant branch, where both assumptions converge into the same P_{rot} solution ($Ro_{\text{crit}} \rightarrow Ro_{\text{TO}}$). The OC stars were used in this work as a consistency check of our models so our statistical tests are only based on field stars.

To find the optimal Ro_{crit} for our sample, all the possible uncertainties were considered (10% error related to SDR, model errors due to stellar parameters and measured P_{rot} errors). The best fit in terms of Ro_{crit} is $2.6_{-0.1}^{+\infty}$, with the corresponding 1σ lower age limit of $t_{\text{crit}} \gtrsim 8.8$, $\gtrsim 6.5$, $\gtrsim 4.2$, and $\gtrsim 2.5$ Gyr for 0.95, 1.00, 1.05 and 1.10 solar mass and metallicity stars, respectively. On the other hand, at 95% confidence level, our result marginally approaches to the solar properties with the Ro_{crit} ranging from 2.3 to Ro_{TO} ($t_{\text{crit}} \gtrsim 5.3$ Gyr, for a solar mass/metallicity star). In all cases, the ΔBIC analysis indicates values greater than +2. For $Ro_{\text{crit},\odot}$, we found $\Delta BIC=+9.2$ indicating a strong evidence favoring the smooth rotation evolution model, at least until the solar rotational level ($\gtrsim 25$ days). For a solar mass star, if the magnetic weakened braking scenario is taking place at these Ro thresholds, we should only detect unusually fast rotators (i.e. stars that depart the gyrochronology relations, considering the measurement errors) at ages considerably older than the Sun (say $\gtrsim 6$ Gyr). Unfortunately, there is a lack of P_{rot} detections in this age range.

Given the statistical difficulties to disentangle the two scenarios, we tend to favor the simplest assumption of the smooth rotational evolution. Other possibility is that maybe the magnetic transition might occur, if it happens at all,

at later evolutionary stages than it was hypothesized before (van Saders et al. 2016). All in all, we conclude with a marginal level of confidence that, considering the available data of solar twins, no indisputable indication emerged about the weakened magnetic braking scenario. On the other hand, we are aware that this phenomenon might be correlated to other manifestations such as drastic changes in stellar cycle morphology and also in stellar differential rotation profile, as some *Kepler* data suggests. For a comprehensive discussion of these possibilities, see Metcalfe & van Saders (2017). Even though, we stress that more data of similar stars is still needed to clarify this issue and firmly establish at what level should we trust on rotation-based ages.

4 CONCLUSIONS

The goal of this paper is to test different rotational evolution scenarios using a selected sample of solar twins characterized with the HARPS, HIRES and GRACES spectrographs. Stellar ages and other evolutionary parameters were estimated through HR diagram analysis with the help of new *Gaia* DR2 G band photometry and parallaxes and precise atmospheric parameters. Measured P_{rot} of 14 solar twins were collected from the literature and/or estimated in this work through Ca II H & K activity time-series. To trace the rotational evolution of solar twins, we build a grid of rotational evolutionary tracks based on modified Kawaler wind law and structural models. We compute these rotation tracks for a large range of critical Rossby number (Ro_{crit}) to account for the magnetic weakened braking phenomena observed by van Saders et al. (2016). We found a marginal statistical evidence favoring the smooth rotation evolution. In the light of magnetic weakened braking scenario, the lower limit of critical Rossby number would be $Ro_{\text{crit}} \gtrsim 2.3$ (at 95% confidence level) which intercepts an age range somewhat older than the Sun and the end of the main-sequence. This result highlights the difficulty to statistically discern both scenarios with the current sample of solar twins. Therefore, it is desirable that other works also approach this issue by determining new P_{rot} of old solar twin stars to clarify the past and the future of the solar rotational evolution.

ACKNOWLEDGEMENTS

We would like to acknowledge the anonymous referee, whose comments have unquestionably led to an improved paper. DLO is grateful to the Brazilian workers and taxpayers, whose effort provided in the past years the stability for young scientists to independently develop their scientific ideas. DLO and JM thanks support from FAPESP (2016/20667-8; 2018/04055-8). LAdS acknowledges the financial support from the European Research Council (ERC) under the European Union's Horizon 2020 research and innovation program (FOUR ACES; grant 724427). MA acknowledges funding from the Australian Research Council (grant DP150100250).

REFERENCES

Angus R., Aigrain S., Foreman-Mackey D., McQuillan A., 2015, *MNRAS*, **450**, 1787

- Barnes S. A., 2007, *ApJ*, **669**, 1167
 Barnes S. A., Weingrill J., Fritzewski D., Strassmeier K. G., Platais I., 2016, *ApJ*, **823**, 16
 Bedell M., et al., 2017, *ApJ*, **839**, 94
 Benomar O., et al., 2018, *Science*, **361**, 1231
 Bilir S., Karaali S., Tunçel S., 2005, *Astronomische Nachrichten*, **326**, 321
 Brandenburg A., Giampapa M. S., 2018, *ApJ*, **855**, L22
 Casagrande L., Ramírez I., Meléndez J., Bessell M., Asplund M., 2010, *A&A*, **512**, A54
 Epstein C. R., Pinsonneault M. H., 2014, *ApJ*, **780**, 159
 Gaia Collaboration et al., 2018, *A&A*, **616**, A1
 Galarza J. Y., Meléndez J., Cohen J. G., 2016, *A&A*, **589**, A65
 Gray D. F., 2005, *The Observation and Analysis of Stellar Photospheres*
 Grieves N., et al., 2018, *MNRAS*, **481**, 3244
 Guerrero G., Smolarkiewicz P. K., Kosovichev A. G., Mansour N. N., 2013, *ApJ*, **779**, 176
 Kawaler S. D., 1988, *ApJ*, **333**, 236
 Krishnamurthi A., Pinsonneault M. H., Barnes S., Sofia S., 1997, *ApJ*, **480**, 303
 Lee-Brown D. B., Anthony-Twarog B. J., Deliyannis C. P., Rich E., Twarog B. A., 2015, *AJ*, **149**, 121
 Liu F., Asplund M., Yong D., Meléndez J., Ramírez I., Karakas A. I., Carlos M., Marino A. F., 2016, *MNRAS*, **463**, 696
 Lorenzo-Oliveira D., Porto de Mello G. F., Schiavon R. P., 2016, *A&A*, **594**, L3
 Lorenzo-Oliveira D., et al., 2018, *A&A*, **619**, A73
 Mamajek E. E., Hillenbrand L. A., 2008, *ApJ*, **687**, 1264
 Mayor M., et al., 2003, *The Messenger*, **114**, 20
 Mazeh T., Perets H. B., McQuillan A., Goldstein E. S., 2015, *ApJ*, **801**, 3
 McQuillan A., Mazeh T., Aigrain S., 2013, *ApJ*, **775**, L11
 Meibom S., et al., 2011, *ApJ*, **733**, L9
 Meibom S., Barnes S. A., Platais I., Gilliland R. L., Latham D. W., Mathieu R. D., 2015, *Nature*, **517**, 589
 Meléndez J., et al., 2017, *A&A*, **597**, A34
 Metcalfe T. S., van Saders J., 2017, *Sol. Phys.*, **292**, 126
 Metcalfe T. S., Egeland R., van Saders J., 2016, *ApJ*, **826**, L2
 Netopil M., Paunzen E., Heiter U., Soubiran C., 2016, *A&A*, **585**, A150
 Noyes R. W., Hartmann L. W., Baliunas S. L., Duncan D. K., Vaughan A. H., 1984, *ApJ*, **279**, 763
 O’Fionnagáin D., Vidotto A. A., 2018, *MNRAS*, **476**, 2465
 Petit P., et al., 2008, *MNRAS*, **388**, 80
 Reiners A., Mohanty S., 2012, *ApJ*, **746**, 43
 See V., et al., 2017, *MNRAS*, **466**, 1542
 Skumanich A., 1972, *ApJ*, **171**, 565
 Spada F., Demarque P., Kim Y.-C., Boyajian T. S., Brewer J. M., 2017, *ApJ*, **838**, 161
 Spina L., et al., 2018, *MNRAS*, **474**, 2580
 Suárez Mascareño A., Rebolo R., González Hernández J. I., Esposito M., 2017, *MNRAS*, **468**, 4772
 Vidotto A. A., et al., 2014, *MNRAS*, **441**, 2361
 Wright N. J., Drake J. J., Mamajek E. E., Henry G. W., 2011, *ApJ*, **743**, 48
 Zechmeister M., Kürster M., 2009, *A&A*, **496**, 577
 do Nascimento Jr. J.-D., et al., 2014, *ApJ*, **790**, L23
 dos Santos L. A., et al., 2016, *A&A*, **592**, A156
 dos Santos L. A., et al., 2017, *MNRAS*, **472**, 3425
 van Saders J. L., Pinsonneault M. H., 2013, *ApJ*, **776**, 67
 van Saders J. L., Ceillier T., Metcalfe T. S., Silva Aguirre V., Pinsonneault M. H., García R. A., Mathur S., Davies G. R., 2016, *Nature*, **529**, 181

This paper has been typeset from a $\text{\TeX}/\text{\LaTeX}$ file prepared by the author.